ISSN 0006-3509, Biophysics, 2018, Vol. 63, No. 3, pp. 469–476. © Pleiades Publishing, Inc., 2018.
Original Russian Text © L.A. Ostrovskaya, D.B. Korman, J.P. Burmiy, V.A. Kuzmin, N.V. Bluhterova, M.M. Fomina, V.A. Rikova, R.R. Guliev, K.A. Abzaeva, 2018, published in Biofizika, 2018, Vol. 63, No. 3, pp. 606–614.

COMPLEX SYSTEMS BIOPHYSICS

An Experimental Study of the Pharmacokinetics of the Antitumor Drug Aurumacryl

L. A. Ostrovskaya[a], *, D. B. Korman[a], J. P. Burmiy[b], V. A. Kuzmin[a], N. V. Bluhterova[a], M. M. Fomina[a], V. A. Rikova[a], R. R. Guliev[a], and K. A. Abzaeva[c]

[a] *Emanuel Institute of Biochemical Physics, Russian Academy of Sciences, ul. Kosygina 4, Moscow, 119334 Russia*
[b] *Institute of Microelectronic Technology and Ultra-High-Purity Materials, Russian Academy of Sciences, ul. Akademika Osipyana 6, Chernogolovka, 142432 Russia*
[c] *Favorsky Irkutsk Institute of Chemistry, Siberian Branch, Russian Academy of Sciences, ul. Favorskogo 1, Irkutsk, 664033 Russia*
**e-mail: larros@list.ru*

Received November 14, 2017; in final form, December 13, 2017

Abstract—The distribution of the antitumor drug aurumacryl (intraperitoneally injected at a dose of 100 mg/kg) in the bodies of animals with Lewis lung carcinoma was studied. The determination of aurumacryl in the tumors and organs (blood, liver, kidneys, lungs, spleen, and brain) of mice was carried out for 48 h by measuring the gold content in the test tissues using inductively coupled plasma mass spectrometry. We found the preferential accumulation of the drug in the kidneys with an extremely low gold content in the brain and a relatively uniform distribution of aurumacryl between the tumor, liver, lung, and spleen tissues.

Keywords: aurumacryl (gold polyacrylate), murine Lewis lung carcinoma, pharmacokinetics, inductively coupled plasma mass spectrometry

DOI: 10.1134/S0006350918030181

Studies of the antitumor properties of metallocenes are actively developing; special attention is paid to the structures that contain noble metals [1, 2].

The interest in organometallic compounds that contain noble metals is largely determined by the discovery of the high level of antitumor activity in a series of complex compounds of platinum (cisplatin, carboplatin, oxaliplatin, etc.) that are widely used in modern chemotherapy of tumors [1, 3].

The accidental discovery of a high level of antitumor activity of *cis*-dichlorodiamine platinum in the late 1960s and then its rapid introduction into clinical practice in the late 1970s drew attention to the possibility of designing novel efficient antitumor agents based on substances that contain transition metals with several degrees of oxidation [4, 5].

It is generally accepted that the main biological effect of such compounds is associated with the central metal. The organic part of the molecule (ligand), which also plays an important role in the effect, provides the stability of the oxidative status of the metal, reduces systemic toxicity, and improves solubility in water. Under physiological conditions, a positively charged metal center is able to bind to negatively charged biomolecules (enzymes and nucleotides) or be reduced. Substantial importance is attached to the nature and degree of oxidation of the metal center, as well as to the types of ligands (donors of oxygen, nitrogen, sulfur, chelating compounds, etc.), which in general provides the coordination geometry of the molecule and its stereochemistry [5].

The development of this area of research led to the discovery of the antitumor activities of organometallic compounds, including another metal of the platinum group, gold.

Gold-containing compounds are considered as promising potential agents for the treatment of malignant tumors. According to the available data, 18 patents for gold-containing compounds with antitumor activities were issued in 2010–2015 [6].

Investigation of the antitumor properties of gold-containing compounds is carried out mainly among complexes that contain gold in the form of monovalent (Au^{1+}) or trivalent (Au^{3+}) ions formed during oxidation of the metal.

Among the huge variety of compounds that contain trivalent gold, dithiocarbamate complexes attract the greatest attention as potential antitumor agents; during their design, it is proposed to create agents that structurally resemble *cis*-dichlorodiamine platinum,

Abbreviations: ICP-MS, inductively coupled plasma mass spectrometry; RB, relative bioavailability.

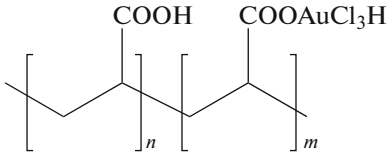

Fig. 1. The structural formula of aurumacryl.

but possess improved properties, such as higher selectivity, bioavailability, and lower toxicity [7].

The antitumor activity of the agent auranofin (gold triethylphosphine), which contains 29% monovalent gold, has been studied in the most detailed way; the agent has already been used in clinical practice for the treatment of rheumatoid arthritis. Clinical trials of auranofin as an antitumor agent in the treatment of chronic lymphocytic leukemia, epithelial ovarian cancer, and non-small cell lung carcinoma have been reported [8, 9].

Significant antitumor activity of a number of the agents that contain gold in the form of complex compounds and nanostructures has been found in vitro against human tumor cell lines, including those resistant to platinum preparations [10–12]. Antitumor activity of some agents was also demonstrated in vivo in a number of tumor models, including xenografts of human tumors (breast, ovarian, and lung cancer, and lymphomas) [8, 13–18].

Differences in the spectrum of antitumor activity, the mechanism of action of compounds that contain gold and platinum, along with a lack of cross-resistance of tumors to some of these agents, give particular relevance to this field of research.

Previously, when studying metal polyacrylates as new compounds for oncology we first detected a significant antitumor activity of the preparation of gold polyacrylate (aurumacryl) [19–21].

Aurumacryl effectively inhibits the growth of murine solid tumors (Lewis lung carcinoma, AKATOL adenocarcinoma, and Ca-755 adenocarcinoma) in vivo by 70–90% compared to the control and causes the death of 60% of MCF-7 human breast carcinoma cells in vitro [22–24].

The data indicate the prospects of further preclinical investigation of aurumacryl as a potential antitumor agent.

It should be noted that aurumacryl occupies a special place in the series of gold-containing compounds that possess antitumor properties; since, unlike other compounds that are "small molecules," it is the first and still the only gold-containing polymer with significant antitumor activity. The use of polyacrylic acid as a carrier when designing a potential antitumor drug is due to the data on the biological activity of this polymer, as a polyanion [25, 26].

The purpose of this work was to study the distribution of aurumacryl in the body of tumor-bearing animals (Lewis lung carcinoma).

MATERIALS AND METHODS

Preparation. Aurumacryl is a partial gold salt of polyacrylic acid that contains 8.03 wt % Au and corresponds to the general formula:

$$(-CH_2-CHCOOH-)_n(-CH_2CHCOOAuCl_3H-)_m,$$

where $n = 1263$, $m = 124$ (Fig. 1).

The molecular weight of aurumacryl is 100–300 kDa. Infrared spectra of the preparation contain absorption bands of the carboxyl and carboxylate groups at 1720 and 1570 cm^{-1}, respectively.

Aurumacryl consists of yellow glassy plates that are readily soluble in water.

The preparation was injected to the animals intraperitoneally at a single dose of 100 mg/kg as an aqueous solution at a volume of 0.2 mL on day 7 after tumor transplantation (tumor mass 0.2–0.4 g).

Laboratory animals. Experiments were performed on BDF_1 inbred male mice with body weights of 18–20 g, which are $f_1(C_{57}Bl/_6 \times DBA_2)$ hybrids of the first generation from the Stolbovaya nursery of the Russian Academy of Sciences (Moscow oblast).

Tumor model. A solid tumor (Lewis lung carcinoma) transplanted subcutaneously by crushed fragments of tumor tissue contained in physiological saline solution to the right side of mice according to the standard procedure was the tumor test system [27]. The inoculum size was 0.3 mL.

Scheme of the experiment. The distribution of aurumacryl in the animals was determined by measuring the gold content in the tumor tissues and the organs (blood, liver, kidneys, lungs, spleen, and brain) of mice using the ICP-MS method.

Biological material was sampled 0.5, 1, 3, 4, 24, and 48 h after the injection of aurumacryl on day 7 after tumor transplantation. We carried out the determination of the mass of tissues extracted for the study, as well as separation of the blood into plasma and serum by centrifugation for 10 min at 3000 rpm.

Similar procedures were performed when studying the control animals that did not receive aurumacryl.

Samples of biomaterial were stored in special marked containers in a freezer at a temperature of −20°C.

Determination of the gold in biological substrates. The determination of the gold in biological materials was carried out using the ICP-MS method in accordance with the previously described procedure [28]. Additionally, a small amount of hydrochloric acid was added to nitric acid to stabilize high concentrations of gold in a solution during autoclave decomposition. Preliminary experiments with the standard tissue sam-

ples (MODAS-3 Herring Tissue and MODAS-5 Cod Tissue) showed that the presence of HCl during autoclave decomposition does not impair the correctness of the determination of all of the certified elements.

Reagents and laboratory glassware. We used deionized water with a resistivity of 18.2 MΩ cm and solutions of single- and multi-element standards (High-Purity Standards, United States). During autoclave decomposition of the samples, concentrated nitric acid (HNO_3 content 65%, max. 0.0000005% Hg, GR, and ISO) and hydrochloric acid were used. Solutions were stored in glass volumetric flasks with a ground stopper in accordance with *GOST* (State Standard) *1770-74* in 15- and 50-mL disposable polyethylene tubes (Labcon, United States; and Deltalab, Spain). All glassware was previously soaked in 5% HNO_3 for at least 4–5 days and washed with deionized water before use.

Equipment. Autoclave decomposition of the samples was carried out in a system of autoclave opening (a development of the Institute of Microelectronic Technology and Ultra-High-Purity Materials of the Russian Academy of Sciences), which is a continuation of the well-proven MKP-05 NPVF system manufactured by ANKON-AT-2 (Russia). The system allows heating of Teflon reaction chambers of a volume of 30 cm^3 to a maximum temperature of 240°C and a pressure of 20 MPa (200 bar). The thermostat block for six autoclaves is equipped with two independent thermocouples and an automatic control unit based on TRM-251 programmable PID temperature controller (OVEN-K, Russia). The control unit makes it possible to perform a five-stage program for thermostat heating, at each step of which the temperature, heating time, and temperature holding time are set.

Mass-spectral determination of the elements was carried out using an X-7 quadrupole mass spectrometer (Thermo Scientific, United States) with the following operating parameters: an output power of the generator of 1300 W, a set of standard nickel cones, a PolyCon concentric nebulizer, a quartz conical spray chamber cooled to 3°C, a flow rate of the plasma-forming argon flow of 13 L/min, a flow rate of the argon auxiliary flow of 0.9 L/min, an argon flow rate in the nebulizer of 0.95 L/min, a sample flow rate of 0.8 mL/min.

Autoclave decomposition of the samples was carried out in batches consisting of five samples with a mass ranging from 100–200 mg and one control sample. Samples were placed in Teflon reaction chamber of autoclaves; 1 mL of HNO_3 and 0.2 mL of HCl were added and the chambers were closed with lids and sealed in titanium enclosures of autoclaves. The autoclaves were placed in an electric heater and heated at 160°C (1 h), 180°C (1 h), and 200°C (0.5 h). After cooling, the autoclaves were opened, the resulting solution was transferred to polyethylene tubes, 0.1 mL of an indium solution at a concentration of 1 mg/L (the internal standard for ICP-MS measurements) was added, and the volume of the solution was adjusted to 10 mL with deionized water. Solutions from Teflon chambers in which the procedures described above were performed without a sample were used as the control.

Processing of results. Calculation of areas under the pharmacokinetic curves (S) was carried out using the trapezium method: each consecutive pair of points on the graph forms a trapezoid. The area under the entire graph was calculated by summing the areas of all trapezoids. Illustrations were performed in the R program using the ggplot2 package [29].

RESULTS

Pharmacokinetic curves that characterize the distribution of aurumacryl in animals with Lewis carcinoma are shown in Fig. 2.

Analysis of these dependencies indicates that after intraperitoneal extravascular injection, aurumacryl was detected in 30 min in the bloodstream, the tumor, and the examined organs (liver, kidneys, lungs, and spleen) of the animals, where it was observed during 48 h of the experiment.

We note that the concentration of gold in the studied tissues in control mice that did not receive aurumacryl is less than 0.006 μg/g.

As can be seen from the data (Fig. 2, Table 1), the maximum concentration of gold (C_{max}) was observed in the blood plasma 3 h after intraperitoneal injection of aurumacryl (Fig. 2a); in the tumor and lungs, after 4 h (Figs. 2b and 2e, respectively); and in the liver, kidneys, spleen, and brain, 24 h after drug administration (Figs. 2c, 2d, 2f, and 2g, respectively).

The values of the minimum concentration of gold (C_{min}) recorded 48 h after drug administration indicate the duration of the residence of aurumacryl in the studied tissues and allow qualitative comparison of the rates of drug excretion from them. As can be seen, the C_{min} indicator increases in the following sequence for organs and tumors: blood plasma –> lungs –> spleen –> tumor –> liver –> kidneys, which indicates an increase in the time of residence of the drug in the tissues in this sequence (Fig. 2, Table 1).

A cumulative pharmacokinetic indicator, namely, the area under the pharmacokinetic curve (S), which makes it possible to evaluate the bioavailability of the tissues of various organs and tumors for aurumacryl, is shown by the data presented in Fig. 3 and Table 1.

In accordance with the values of this integral indicator of organ bioavailability for aurumacryl, the increase in gold content in various tissues occurs in the following sequence: brain –> blood plasma –> lungs –> spleen –> tumor –> liver –> kidneys (Fig. 3, Table 1).

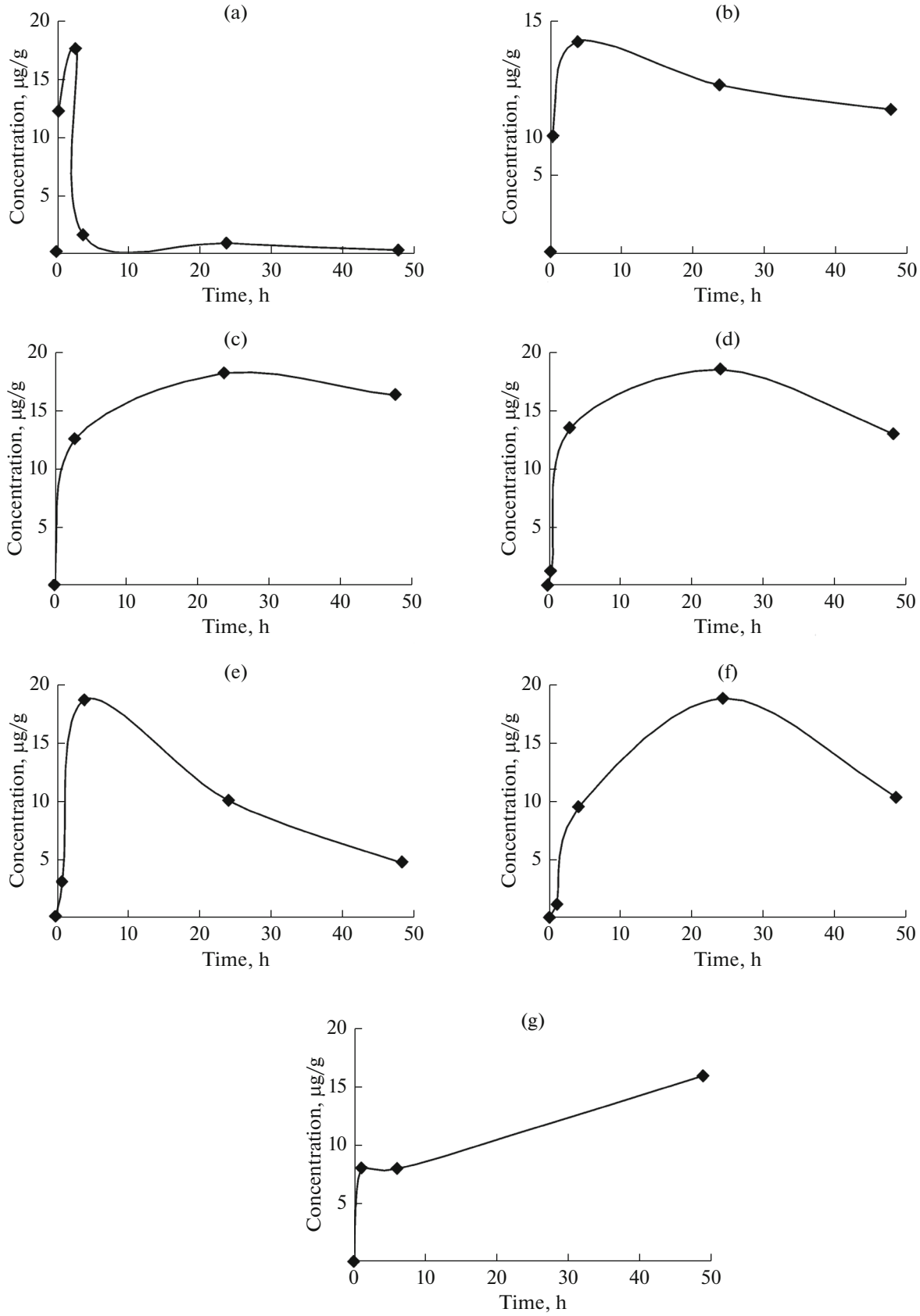

Fig. 2. The kinetics of change in the gold content in (a) blood plasma, (b) tumor, (c) liver, (d) kidney, (e) lungs, (f) spleen, and (g) brain in mice with Lewis lung carcinoma after a single intraperitoneal injection of aurumacryl at a dose of 100 mg/kg.

Table 1. The pharmacokinetic parameters of aurumacryl distribution in animals with Lewis lung carcinoma (intraperitoneal injection at a dose of 100 mg/kg)

Tissue samples	C_{max}, μg/g	T_{max}, h	C_{min}*, μg/g	S, μg/(g h)	RB factor
Blood plasma	15.6	3	0.9	88.1	–
Tumor	13.6	4	9.2	522,8	5.93
Liver	14.5	24	13	602.2	6.83
Kidneys	129.0	24	90	5099	57.87
Lungs	14.0	4	3.5	372.6	4.23
Spleen	13.1	24	7.2	452.1	5.13
Brain	0.36	24	–	6.8	0.08

* The minimum values of gold concentration recorded 48 h after aurumacryl administration.

It is noteworthy that aurumacryl was detected in extremely low concentrations in the brain; the order of magnitude was lower than the concentration recorded in plasma (Figs. 2 and 3, Table 1). Such a low gold content in the brain tissues indicates that the drug is not able to overcome the blood–brain barrier.

Thus, these data indicate the preferential accumulation of the drug in the kidneys with a relatively uniform distribution of aurumacryl between the tissues of the tumor, liver, lungs, and spleen.

The relative bioavailability (RB) factor of tissues of various organs and tumors for aurumacryl, which is defined as the ratio between the areas under the curves for the organ (S_o) under examination or the tumor and blood (S_b): $RB = S_o/S_b$, also indicates the predominant accumulation of aurumacryl in the kidneys.

The value of the RB factor for the kidneys is an order of magnitude higher than for all other organs (liver, lungs, and spleen) and tumors (Fig. 2, Table 1).

The observed high bioavailability of the kidneys to aurumacryl indicates a definite tropism of the drug to the kidney tissues and suggests that the kidneys may be a potential target of both the antitumor and toxic effects of the drug.

At the same time, it seems appropriate to note that nephrotoxicity is one of the main undesirable toxic side effects of antitumor drugs of the platinum group, which limits their use [1].

The selective accumulation in the kidneys that was found when studying the pharmacokinetics of nitrulline, a chemotherapeutic agent that belongs to the group of alkylnitrosoureas, was subsequently reflected in the manifestation of its nephrotoxicity, as revealed during clinical trials of the drug [30].

It should be mentioned that another drug of the class of alkylnitrosoureas, methylnitrosourea, which is one of the most efficient agents in the chemotherapy of lung tumors showed a high tropism to the tissues of the lungs in an experimental study of its pharmacokinetics [30].

When considering the data on the bioavailability of aurumacryl for the tumor, it should be noted that the drug was detected in a subcutaneously developing tumor almost simultaneously with the entry of the substance into the blood after extravascular intraperitoneal administration; it was recorded at the maximum concentration after 3 hours and it remained in tumor tissues at a concentration close to the maximum one during the entire observation period of 48 h (Fig. 1, Table 1).

As mentioned earlier, the relative bioavailability of the tumor to aurumacryl is approximately the same as for the other studied organs (with the exception of the kidneys with the highest RB index and the brain with the lowest RB factor). However, numerically, the RB factor for the tumor (5.93) is slightly higher than the RB values found for the spleen (5.13) and the lungs (4.23), but lower than the RB value recorded for the liver (6.83) (Fig. 2, Table 1).

The established value of the RB coefficient of the tumor for aurumacryl corresponds to the values of this index for a number of other antitumor drugs, which vary in the range from 1.6 to 10.5 [30].

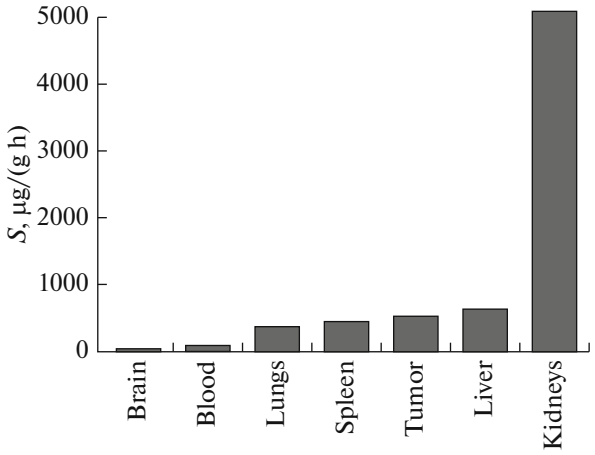

Fig. 3. The areas under the pharmacokinetic curves (S) that characterize the bioavailability of the tumor and organs of animals with Lewis lung carcinoma for aurumacryl.

Thus, the study of the distribution of the potential antitumor agent aurumacryl in the body of tumor-bearing animals (Lewis lung carcinoma) made it possible to establish that aurumacryl, after intraperitoneal injection, enters the bloodstream, organs (liver, kidneys, lungs, and spleen) and the tumor, where it was found throughout the 48-h observation period.

DISCUSSION

Investigation of the pharmacokinetics of new pharmaceutical agents is a mandatory step in their study, which is important for the development of optimum modes and regimens of application of drugs, as well as for understanding the mechanisms of their action.

The pharmacokinetics of gold-containing compounds with antitumor activity had not been studied.

The exception is auranofin, whose pharmacokinetics were determined during study of this compound as an anti-rheumatoid agent that exhibits an anti-inflammatory effect. It was shown that auranofin used at a daily dose of 6 mg is absorbed from the gastrointestinal tract at 25%, while 60% of the drug binds to blood plasma proteins. Auranofin undergoes rapid metabolism in the liver and is practically not determined in an unchanged form in the blood. The equilibrium concentration of the drug in the blood is 68 μg/mL; it is achieved 3 months after the start of treatment. The elimination half-life ($t_{1/2}$) of the drug from the blood is 21–31 days and 42–128 days from the tissues of organs. Most of the auranofin (approximately 60%) is excreted through the kidneys with urine; the rest is excreted with bile.

The pharmacokinetics of auranofin in humans was also studied during the first phase of clinical trials of the drug as an antiparasitic agent. The study included 15 healthy volunteers who received the drug orally at 6 mg per day for 7 days. The contents of the drug in blood plasma and feces were determined by detection of gold using an ICP-MS method similar to that used in our study. The average maximum concentration of gold (C_{max}) in the blood on the 7th day was 0.312 mg/mL; elimination half-life ($t_{1/2}$), 35 days. After the first day, gold was not detected in feces; on the 7th day the average concentration of gold was 8.8 mg/g, from which it was calculated that ~64% of the administered dose was excreted with feces in 7 days [31].

Our study of the pharmacokinetics of aurumacryl (containing trivalent gold polyacrylate) showed that aurumacryl is absorbed from the abdominal cavity and enters the bloodstream. In the examined organs (liver, kidneys, lungs, and spleen) and tumors, gold was detected 30 min after intraperitoneal administration and continued to be determined during the 48 h of the observation.

Analysis of the data we obtained shows that an approximately uniform distribution of gold between tissues of the tumor, liver, and spleen occurred. The elimination of gold from the lungs is faster than from the tumor and other organs. Attention is given to the significantly greater accumulation of gold in the kidney tissue, which can be interpreted as the fact that the drug is excreted from the body mainly with urine. The very low gold content in the brain tissue obviously indicates the impossibility of penetration of the polymer agent through the blood–brain barrier.

The study of the drug metabolism in the body, along with the identification of active metabolites and pathways of their interaction with biomacromolecules, are of great importance for understanding the mechanisms of their action. Gold polyacrylate, as an effective haemostatic, has a high specificity of interaction with the albumin molecule and forms an interpolymer complex [32]. It can be assumed that in tumor-bearing animals after entering the bloodstream aurumacryl binds to blood serum albumins and enters the tissues as a complex with albumin, where further interaction of this complex with intracellular macromolecules occurs. Obviously, the processes of biodegradation and aurumacryl metabolism should be the subject of special studies.

No selective accumulation of metal in any of the studied tissues or noticeable lesion of any organ, including the kidneys, was found during the toxicological study of dithiocarbonate complexes that contain trivalent gold [5].

The data obtained in the present work on the distribution of gold in tumor-bearing animals after administration of aurumacryl should be considered in a special in-depth preclinical toxicological study of the agent.

In considering the possible mechanisms of the antitumor activity of gold-containing agents, we note that the characteristic chemical properties of these compounds, which are caused by the gold atom, determine their particular pharmacological profile and mechanism of action.

The experimental results obtained thus far indicate that the mechanism of action of gold-containing agents is different from that of most known antitumor agents, including cisplatin derivatives. According to the available data, DNA is not the main and exclusive target for the cytotoxic effect of these compounds, in contrast to the targeting of platinum preparations [12–14].

A number of cellular proteins that can play a role in tumor growth are indicated as the most likely targets for the antitumor effect of gold preparations [11].

As shown in a number of studies, one of the targets for gold-containing compounds is the "thioredoxin–thioredoxin reductase" system that regulates the level of reactive oxygen species in the cytosol and mitochondria. The inhibition of mitochondrial thioredoxin reductase that is induced by gold-containing compounds leads to an increase in the level of mito-

chondrial reactive oxygen species in the mitochondria, a violation of the permeability of mitochondrial membranes, and release of cytochrome *c* and the apoptosis-inducing factor into the cytosol, which results in apoptotic cell death via the mitochondrial pathway. Selective inhibition of thioredoxin reductase activity is caused by the high affinity of gold for selenium, which is part of the active site of this enzyme with the formation of Au–Se bonds [15, 18, 33, 34].

Based on such ideas, it is possible to consider gold-containing compounds as a new group of potential antitumor drugs with a pro-oxidant effect.

Other possible mechanisms of the antitumor effect of these compounds have been observed in a number of experiments, among which are inhibition of proteasome 26S, influence on proteins involved in apoptosis, DNA intercalation, influence on the topoisomerase I-mediated untwisting of the DNA strands, and an anti-angiogenic effect [10, 11, 13, 35–39].

These issues show that gold-containing compounds are potential antitumor agents with a multitarget mechanism of action that has been investigated [40, 41].

CONCLUSIONS

The distribution of aurumacryl in the body of tumor-bearing animals after intraperitoneal injection at a dose of 100 mg/kg on day 7 of the development of Lewis lung carcinoma was studied.

The determination of aurumacryl in the tumor and organs (blood, liver, kidneys, lungs, spleen, and brain) of mice was carried out for 48 h by measuring the gold content in the test tissues using the ICP-MS method.

It was found that 30 min after intraperitoneal extravascular injection, the agent was observed in the bloodstream, tumor, and the test organs (liver, kidneys, lungs, and spleen) of animals, where it was detected during the entire 48-h observation period.

The maximum concentration of gold was observed in the blood plasma 3 h after the drug administration; in the tumor and lungs, in 4 h; in the liver, kidneys, spleen, and brain, in 24 h.

It was shown that the area under the pharmacokinetic curve, which characterizes the bioavailability of tissues of various organs and tumors for aurumacryl, increases in the following sequence: brain → blood plasma → lungs → spleen → tumor → liver → kidneys.

The parameter of the relative bioavailability of the tumor to aurumacryl is approximately at the same level as for the other studied organs (with the exception of the kidneys, with the highest RB index, and the brain, with the lowest RB index). However, the RB index for the tumor is numerically somewhat higher than the RB values found for the spleen and lungs, but slightly inferior to the RB value registered for the liver.

These data indicate the preferential accumulation of the drug in the kidneys, with an extremely low gold content in the brain and a relatively uniform distribution of aurumacryl between the tissues of the tumor, liver, lungs, and spleen.

ACKNOWLEDGMENTS

The work was financially supported by the Ministry of Education and Science of the Russian Federation (project no. 14.607.21.0199 Development of a technology for obtaining a drug based on nanostructured gold polyacrylate for molecular-targeted tumor therapy in the framework of the Federal Target Program Research and Development in Priority Areas for the Development of Russia's Science and Technology Complex for 2014–2020 (Agreement no. 14.607.21.0199 dated September 26, 2017; unique code RFMEFI61315X0042).

REFERENCES

1. D. B. Korman, *Fundamentals of Antitumor Chemotherapy* (Prakticheskaya Meditsina, Moscow, 2006) [in Russian].
2. V. N. Babin, Yu. A. Belousov, V. I. Borisov, et al., Izv. Akad. Nauk, Ser. Khim., No. 11, 2405 (2014).
3. I. A. Efimenko, Koordnats. Khim. **24** (4), 282 (1998).
4. M. Frezza, S. Hindo, D. Chen, et al., Curr. Pharmacol. Des. **16**, 1813 (2010).
5. C. Nardon, F. Chiara, L. Brustolin, et al., Chem. Open **4,** 183 (2015).
6. C. Nardon, N. Pettenuzzo, and D. Fregona, Curr. Med. Chem. **23**, 3374 (2016).
7. L. Ronconi and D. Fregona, Dalton Trans. **48**, 10670 (2009).
8. X. Chen, X. Shi, X. Wang, and J. Liu, Cancer Cell Microenviron. **1**, 415, (2014).
9. D. Oomen and D. Yiannakis, Mutat. Res. 784–785, 8 (2015).
10. D. Saggioro, M.P. Rigobello, L. Paloschi, et al., Chem. Biol. **14,** 1128 (2007).
11. S. Nobili, E. Mini, I. Landini, et al., Med. Res. Rev. **30,** 550 (2010).
12. A. Markowska, B. Kasprzak, K. Jaszczynska-Nowinka, et al., Contemp. Oncol. (Poznan) **19**, 271 (2015).
13. A. Casini and L. Messory, Curr. Top. Med. Chem. **11**, 2647 (2011).
14. I. Kostova, Anticancer Agents Med. Chem. **6**, 19 (2006).
15. E. Topkas, N. Gai, A. Cumming, et al., Oncotarget **7**, 831 (2016).
16. V. Gandin, A. P. Ferhanes, and M. P. Rigobello, Biochem. Pharmacol. **79**, 90 (2010).
17. L. Cattaruza, D. Fregona, M. Mongiat, et al. Int. J. Cancer **128**, 202 (2011).
18. G. Marzano, V. Gandin, A. Fold, et al. Free Radic. Biol. Med. **42**, 872 (2007).
19. M. G. Voronkov, K. A. Abzaeva, L. V. Zhilitskaya, et al., RF Patent No. 2372091 (May 20, 2008).

20. L. A. Ostrovskaya, M. G. Voronkov, D. B. Korman, et al., J. Cancer Ther. **1** (2), 59 (2010).
21. L. A. Ostrovskaya, D. B. Korman, N.V. Bluhterova, et al., Biointerface Res. Appl. Chem. **4 (**4), 816 (2014).
22. L. A. Ostrovskaya, M. G. Voronkov, D. B. Korman, et al., Biophysics (Mosow) **59 (**4), 642 (2014).
23. L. A. Ostrovskaya, A. K. Grehova, D. B. Korman, et al., Biophysics (Mosow) **62** (3), 485 (2017).
24. L. A. Ostrovskaya, D. B. Korman, A. K. Grehova, et al., Izv. Akad. Nauk, Ser. Khim., No. 12, 2333 (2017).
25. T. Suzuki, K. Sarai, K. Kohda, and Y. Kawazoe, Anticancer Res. **11 (**2), 953 (1991).
26. N. A. Plate and E. A. Vasil'ev, *Physiologically Active Polymers* (Khimiya, Moscow, 1986) [in Russian].
27. E. M. Treshchalina, O. S. Zhukova, G. K. Gerasimova, et al., *Guidelines for Experimental (Preclinical) Study of New Pharmacological Substances*, Ed. by R. U. Khabriev (Meditsina, Moscow, 2005) [in Russian].
28. V. K. Karandashev, T. A. Orlova, A. E. Lezhnev, et al., Inorg. Mater. **44 (**14), 1491 (2008).
29. H. Wickham, *ggplot2: Elegant Graphics for Data Analysis* (Springer, New York, 2009).
30. L. A. Ostrovskaya, V. A. Filov, B. A. Ivin, et al., Ross. Bioterapevt. Zh. **3** (1), 37 (2004).
31. E. V. Caparelli, R. Bricker-Ford, M. J. Rogers, et al. Antimicrob. Agents Chemother. **61** (1), e01947-16. (2017). doi doi 10.1128/AAC-01947-16
32. K. A. Abzaeva, L. V. Zhilitskaya, G. G. Belozerskaya, and L. A. Ostrovskaya, Izv. Akad. Nauk, Ser. Khim., No. 12, 2314 (2017).
33. Y. Liu, Y. Li, S. Yu, and G. Zhao, Curr. Drug Targets, **13**, 1432 (2012).
34. S. M. Meier, C. Gerner, B. K. Keppler, et al., Inorg. Chem. **255**, 4248 (2016).
35. X. Zhang, M. Frezza, V. Milacic, et al., J. Cell Biochem. **109**, 162 (2010).
36. T. Zou, C. T. Lum, C. N. Loc, et al., Chem. Soc. Rev. **44**, 8786 (2015).
37. S. Perez, C. deHaro, Vicente C., et al., ACS Chem. Biol. (2017). doi 10.1021/acschembio7600090
38. A. Casini, G. Kelter, C. Gabbiani, et al., J. Biol. Inorg. Chem. **14**, 1139 (2009).
39. C. Gabbiani, A. Casini, G. Ketler, et al., Metallomics **3**, 1318 (2011).
40. M. Celegato, D. Fregona, M. Mongiat, et al., Future Med. Chem. **6**, 1249 (2014).
41. C. Nardon, G. Boscutti, and D. Fregona, Anticancer Res. **14**, 487 (2014).

Translated by G. Levit